RSC Advances

ROYAL SOCIETY OF CHEMISTRY

www.rsc.org/advances

Surface morphology and corresponding electrochemistry of polypyrrole films electrodeposited using water miscible ionic liquid

Maria Grzeszczuk[a], Rabia Ozsakarya[b]

Faculty of Chemistry, University of Wrocław, 14 F. Joliot-Curie, 50-383 Wrocław, Poland

Abstract

Polypyrrole layers were deposited on polycrystalline gold from solutions of pyrrole in ionic liquid 1-butyl-3-methylimidazolium tetrafluoroborate and its equimolar mixture with water by using potential controlled electrochemical methods. Cyclic voltammetry, electrochemical impedance spectroscopy, scanning electron microscopy and dispersive X-ray microanalysis were characterization methods of polymeric products. Morphology of the solution side of the polymer layers depended on composition of the polymerization bath and layer thickness. Correlations between impedance parameters and surface morphologies were investigated.

Intermolecular interactions in the ionic liquid and in its mixture with water were invoked to discus packing motifs of the polypyrrole chains deposited on gold. Different morphologies of the polypyrrole films, from a crystal-like solid to a colloid semi-rigid liquid, were observed for the submicrometer films. Values of the double layer impedance frequency dispersion parameter as well as elemental microanalysis data are consistent with the surface morphology images. The charge transport processes of polypyrrole electrode are impacted by morphology as well as thickness of the thin polymer films.

The ionic liquid electrolytes can be used to tailor the micro and nanostructures of electrodeposited polypyrrole.

---

[a] Corresponding Author, e-mail: maria.grzeszczuk@chem.uni.wroc.pl , tel. 48 71 3757336
[b] LLP Erasmus 2011/2012 student at University of Wrocław; on leave from Suleyman Demirel University, Chemistry Department, 32260 Isparta, Turkey; e-mail: rabiaozsakarya@gmail.com.

<u>*Key words:*</u> 1-butyl-3-methylimidazolium tetrafluoroborate, electrochemical polymerization and characteristics, surface morphology and composition

Introduction

Many molecular solvents have been used to electropolymerize pyrrole. The most common are water and acetonitrile because their low enough nucleophilicity is protecting the polymer against degradation processes. Great differences were found for polypyrrole synthesized in dry acetonitrile when compared to one prepared in acetonitrile-water mixed solvent. The water effect concerns acceleration of the electropolymerization process as well as impacting of properties of the polymer [1]. Later on, the air and moisture-stable ionic liquids with 1,3-dialkyl immidazolium cations became popular electropolymerization media as their use resulted in significantly altered film morphologies and improved electrochemical activities of polypyrrole [2-4]. Therefore, the goal of this work is to present electrochemical and specific microscopic appearences of the polypyrrole films due to the hydroscopic 1-butyl-3-methylimidazolium tetrafluoroborate (BMIMBF$_4$) solvent. Miscibility of BMIMBF$_4$ and H$_2$O might highly impact electropolymerization process thus resulting in new properties of the polypyrrole films.

The research activity in the field of ionic liquids or room temperature ionic liquids (ILs or RTILs) has increased dramatically during the last years. Also their use as an environmentally friendly alternative for conventional solvents has gained much attention in electrochemical research and applications [5]. Room temperature ionic liquids have been presented in chemistry as a new class of solvents for extraction processes and organic reactions, both for catalyzed and uncatalyzed [6]. The organic molten electrolytes, especially those at or near ambient temperature, have been the focus of many scientific investigations since a long time because of their specific physical and chemical properties [7]. Ionic liquid solvents with non-flammability and non-volatility can dissolve a wide range of organic and

inorganic compounds. For usefulness in electrochemistry high ionic conductivity, good thermal stability and a wide electrochemical window should characterize them [8].

In recent years, ILs have been used in polymer science, mainly as polymerization media in several types of polymerization processes, including conventional free radical polymerization [9]. Furthermore, as electrolytes with wide potential windows and high ionic conductivity, the air and moisture stable ILs are expected to be peculiarly suitable medium for electropolymerization and applications in π-conjugated polymer electrochemical devices [10].

The properties of ionic liquids can be adjusted by choosing specific combinations of cations and anions. For instance, they can be made either hygroscopic or hydrophobic. The number of already described and potential cation–anion combinations is very large. Typically ionic liquids are composed of bulky 1,3-dialkylimidazolium, alkylammonium, alkylphosphonium or alkylpyridinium organic cations and inorganic anions such as most frequently $AlCl_4^-$, BF_4^- or PF_6^- but also NO_3^-, ClO_4^-, CF_3COO^-, $CF_3SO_3^-$ or CH_3COO^- and other anions. The most commonly known ionic liquids include 1-butyl-3-methylimidazolium hexaflurophosphate and tetrafluroborate abbreviated as $BMIMPF_6$ and $BMIMBF_4$, correspondingly. However the two salts differ substantially regarding miscibility with water. In this study, water miscible $BMIMBF_4$ was used. Electropolymerization of pyrrole and subsequent characterization of the resulting polymer in $BMIMBF_4$ environment were not yet reported to the best of our knowledge. A general advantage of using the ionic liquid solvents over other electrolytes for electropolymerization and subsequent electrochemical processing might result from their wide potential and temperature windows.

A main purpose of this study was to carry out electrooxidative polymerization of pyrrole in the ionic liquid using the potentiostatic and cyclic potentiodynamic electrolytic regimes and investigate influence of the electrolyte on properties of the polymer electrode using cyclic voltammetric (CV) and impedimetric (EIS) characterization of the

electrodeposited polypyrrole (PPy). Scanning electron microscopy (SEM) images of the resulting polymer electrodes were taken to reveal their surface morphology and energy dispersive X-ray (EDX) elemental microanalysis was used as well. Furthermore, an influence of water added to the electropolymerization medium on the electrochemical performance of the polymer was followed. So far, no reports have appeared on redox and impedance characteristics of a conducting polymer electrodeposited in presence of and without water in a liquid salt. Consequences of polypyrrole deposition in $BMIMBF_4$ (freshly dried or after storage) and in equimolar $BMIMBF_4$-H_2O solution on electrochemical characteristics (CV, EIS) of the polymer films in $BMIMBF_4$ as well as on their corresponding surface morphology (SEM) and composition (EDX) are shown.

2. Materials and Methods

2.1. Chemicals

Pyrrole (Aldrich) was distilled in an atmosphere of nitrogen under reduced pressure before use in the electrode cell and was stored in a freezing compartment to protect against the action of light and oxygen. $BMIMBF_4$ (Aldrich) was dried under vacuum at 70 °C for one day just before using in the electrooxidative polymerization of pyrrole (session 1) or after storage of the dried liquid salt in a freezer for a few weeks (session 2). Ultrapure water (Millipore) was used to prepare equimolar $BMIMBF_4$- H_2O mixtures.

2.2. Preparation of substrate electrodes

The polycrystalline gold electrodes (Au1, Au2, Au3 and Au4) chosen for the experiments was subjected to mechanical, chemical and electrochemical pretreatments before electrodeposition of polypyrrole. At first, the polycrystalline gold surface were polished with the 10, 3, 1 and 0,3 μm aluminum oxide powders (Aldrich, Alfa Aesar), starting from the biggest oxide particle powder and finishing with the smallest one. The each polishing step

was taking 10 min and it was followed by sonification in the demineralized water to wash out the powder particle from the surface. Later on, the chemical cleaning was carried out in Piranha solution (30% H_2O_2 + 95% H_2SO_4; 1:3 v/v) for 5 min. Finally, the cyclic voltammetry was performed at the scan rate 0.1 V/s, in deoxygenated 0.5 M H_2SO_4, in the potential range (-0.1V, +1.4V) *vs.* Ag/AgCl/Cl$^-$(sat.) for the electrochemical cleaning/activation of Au by the multicyclic oxidation/reduction process. After rinsing in water the electrodes were stored in a desiccator.

2.3. Polymerization processes

The polymerization of pyrrole was carried out by a cyclic potentiodynamic method (CV) and a potentiostatic method (chronoamperometry, CA). A standard three electrode cell was used. The working electrode was polycrystalline gold electrode, the auxiliary electrodes were platinum plate, Pt rod or Pt leaf and the pseudo-reference electrode was Ag wire. $BMIMBF_4$ was used at a room temperature. The pure nitrogen (Azot 6.0) was utilized during all of measurements to protect the liquid from air.

Four gold electrodes (Au1, Au2, Au3, Au4) were used in two polymerization sessions. Before polymerization, the potential window of Au in the ionic liquid was checked in. After the potential window was determined, 0.07 ml pyrrole was put into 10 ml volume of the ionic liquid to give 0.1 M monomer solution concentration, which corresponds to 0.02 molar quotient of pyrrole in $BMIMBF_4$.

In a first synthesis session, Au2 and Au3 were used to produce polypyrrole with the potentiodynamic method, Au4 was used with the potentiostatic method and Au1 was used with a combination of the both methods. Then the samples were designated as Au2/PPy, Au3/PPY, Au4/PPy and Au1/PPy, respectively. Au4/PPy was obtained in a multistage procedure, which started and ended with potentiostatic depositions at 1.0 V and 1.2 V respectively. Au1/PPy was obtained under successive potentiostatic at +0.9V for 1000s and

5

(-0.65,+1.1)V at 0.05V/s CV regimes, 80 scans: Au3/PPy was prepared under (-0.55,+1.1)V

CV at 0.1V/s, 100 scans: Au2/PPy was prepared under (-0.65,+1.1)V CV at 0.1V/s, about 100

scans.

In a second synthesis session, only three substrate gold electrodes were used: Au2 and

Au3 for the potentiodynamic syntheses in potential range (-0.6 V, +1.1 V), and Au4 for the

step by step potentiodynamic syntheses in the potential ranges from -0.6 V to +0.8V, +0.9 V

and +1.0 V in the three successive steps, respectively. Then the later samples were designated

as Au2a/PPy, Au3a/PPy and Au4a/PPy, respectively. Note that the legends of the Figures and

Tables contain description of the synthesis relevant to the data reported there. Amount of

electric charge consumed for the polymer deposition differed from sample to sample but was

not larger than 0.3 C/cm^2 (8.9 mC/0.03 cm^2) and thus corresponded to thickness of the order

of 10^{-1} μm for the most PPy films, except for Au4/PPy where it was of the order of $1 \cdot 10^0$ μm

[11,12].

After each polymerization the electrodes were washed with acetonitrile to remove the

ionic liquid remaining into the polymer films and then dried at room temperature in a

desiccator.

2.4. Characterization of polypyrrole films

Dc and ac electrochemical processes were run using the Autolab-PGSTAT20

apparatus consisted of GPES and FRA measurement-software modules (v. 4.8), respectively.

Cyclic voltammograms of the electrodeposited polypyrrole samples in BMIMBF$_4$ were done

at 0.01, 0.02, 0.05 and 0.10 V/s, before and after the EIS spectra measurements to check

redox stability of the polymer. The EIS measurements were performed with 10 mV amplitude

of the sinusoidal excitation at frequencies from 50 kHz to 100 mHz or to 1mHz or, most

commonly, to 5 mHz at different dc potentials (-0,4, 0,2, 0,8, 1,2 V).

Later on, *ex-situ* SEM images of the polypyrrole electrodes were made using HITACHI S-3400 N scanning electron microscope. The X-ray (EDX) microanalysis method for quantitative characterization of the polymer films was inspected as well.

3. Result and discussion

3.1. Electrodeposition and performance in dry BMIMBF$_4$

Potentiostatic depositions were done at potentials 0.9, 1.0 and 1.2 V. Chronoamperograms, compared in Fig.1 point out a kinetic regime of electrodeposition. In general, the recorded current-time curves are composed of the double layer, monomer polymerization and polymer oxidation currents. The former contribution is often negligible on a longer time scale when the potentiostatic current reaches a stationary value of the 3D polymer growth [13]. The pyrrole polymerization produces protons and polypyrrole oxidation always involves anions. Therefore, diffusion of pyrrole, protons and counter-ions must be of importance for the rate of the electrochemical deposition process [14]. Cyclic potentiodynamic electropolymerization have been done with potential scan rate 0.100 V/s and encompassed potential windows *c.a.* (-0.6,+1.1)V. A selection of scans recorded during the potentiodynamic growth is shown in Fig. 2.

Figure 1.

Figure 2.

The products of the two fore mentioned polymerization procedures were characterized by CV and EIS [11]. Voltammograms of the three independent polymer samples are shown in Fig. 3. The redox activity measured as a mean anodic/cathodic charge involved in the redox switching, when assumed to correlate with a yield and thickness of polypyrrole, indicate the following order of polymer layer thickness: Au1/PPy>Au3/PPy>Au2/PPy.

Figure 3.

Electrochemical impedance spectra of the polypyrrole films being under comparison were collected in the same frequency regions containing the same number of frequency data points, at electrode potentials corresponding to different reversible oxidation levels of the polymer. The (100 kHz, 5 mHz) spectra for the PPy samples oxidized at +0.2 V are compared in Fig. 4. Changes in the impedance magnitude follow that evidenced by the cyclic voltammograms thus resulting mainly from differences in the polymer layer thickness. In general, the imaginary component of the impedance decreases with thickness as a consequence of an increased capacitance of the film. The lowest frequency Z" values bear a dominant contribution from the redox pseudocapacitance of polypyrrole. Thus so, a higher capacitance (a lower Z") is observed for a thicker film. The higher frequency ranges of the spectra, shown in the bottom of Fig. 4, point out more resistive impedance of the Au3/PPy as compared with thicker (Au1/PPy) and thinner (Au2/PPy) films. Remarkably, no parts of the spectra in this range resembles the pure Warburg impedance behavior, which means fast ionic diffusion and/or special diffusion paths similar to that observed for a crystalline oxide material [12].

The EIS data can be analyzed on a quantitative basis using the equivalent electrical circuit approach. The ladder type circuit structure was assumed for the polypyrrole electrode and, using the Boukamp's circuit code, the experimental data were fitted to the $R_0(Q_1[R_1(Q_2T)])$ circuit shown also in scheme 1 [15].

Scheme 1. Electrical circuit model of the electrochemical cell
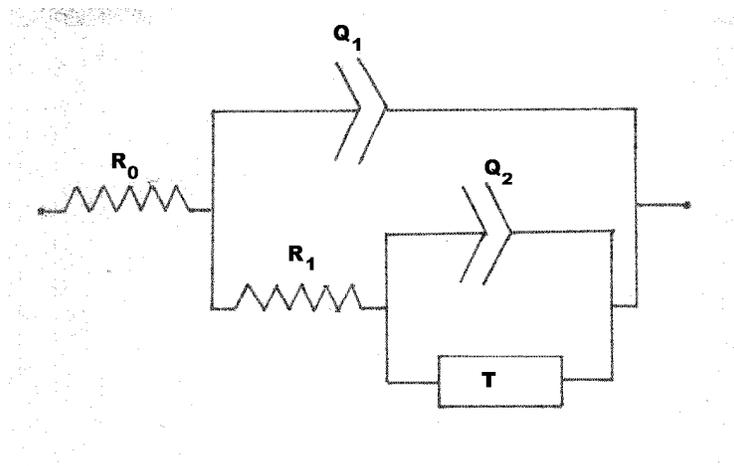
There, R_0 is the electrolyte resistance (ionic liquid), R_1 is the charge transfer resistance of the polymer electrode (ionic liquid / polypyrrole film interface), Q_1 and Q_2 are the constant phase elements – the general diffusion related frequency dispersions corresponding to fast (double layer) and slower (adsorption) processes of the polymer electrode, respectively. T is the finite length diffusion element characteristic for diffusion through a medium where one boundary is blocking for the diffusing species (Au surface blocks ions diffusing through the polymer). The frequency dispersion admittance functions of elements Q and T are as follows, respectively [15]:

$$Y_Q = Y_{0,Q} \cdot (j\omega)^n \qquad \text{with } 0<n<1 \qquad (1)$$

$$Y_T = Y_{0,T} \cdot \sqrt{j\omega} \cdot \tanh(B\sqrt{j\omega}) \qquad (2)$$

where: $Y_{0,Q}$ and n as well as $Y_{0,T}$ and B are parameters of Y_Q and Y_T, respectively. The imaginary value $j = (-1)^{1/2}$.

The parameters of the best CNLS (complex nonlinear least squares) fits of the experiment – simulation data are collected in Table 1.

Table 1. Impedance/admittance parameters of polypyrrole electrodes prepared and measured in dry BMIMBF$_4$. CV deposition of Au2/PPy and Au3/PPy; CA + CV deposition of Au1/PPy. The order of thickness is Au2/PPy<Au3/PPy<Au1/PPy. The CNLS fitting with the electrical circuit model gives the χ^2-values of the order of 10^{-4}. Relative errors of parameters are depicted in italics.

Parameter / electrode	Au2/PPy	Au3/PPy	Au1/PPy
R_0 / kΩ	0.64 *2%*	1.30 *1%*	0.77 *1%*
R_1 / kΩ	3.67 *4%*	33.4 *2%*	2.21 *4%*
$Y_0(Q_1)$ / $\Omega^{-1}s^{+n}$	$1.6 \cdot 10^{-6}$ *12%*	$0.9 \cdot 10^{-6}$ *3%*	$3.5 \cdot 10^{-6}$ *10%*
$n(Q_1)$	0.65 *2%*	0.61 *1%*	0.63 *2%*
$Y_0(Q_2)$ / $\Omega^{-1}s^{+n}$	$4.7 \cdot 10^{-6}$ *6%*	$4.9 \cdot 10^{-6}$ *1%*	$7.3 \cdot 10^{-6}$ *7%*
$n(Q_2)$	0.77 *1%*	0.60 *<1%*	0.74 *2%*
$Y_0(T)$ / $\Omega^{-1}s^{+1/2}$	$1.3.0 \cdot 10^{-6}$ *10%*	$0.7 \cdot 10^{-6}$ *9%*	$5.7 \cdot 10^{-6}$ *3%*
$B(T)$ / $s^{1/2}$	1.0 *5%*	3.4 *5%*	1.9 *1%*

One should note that the most impedance parameters for the thinnest of these films (Au2/PPy) are similar to those of the much thicker film prepared by the sequential method (Au1/PPy). The impedance characteristics of the three films seem to originate from their thickness and surface morphology. The possibly lowest effective surface area of the Au3/PPy film may be related to the biggest size of the polymer particulates at the surface of the electrolyte (compare Figs. 5 and 6). So, the smaller particles enhance the interfacial ion transfer and impact the bulk film conductance processes by lengthening the ionic diffusion paths.

Figure 4.

3.2. Surface morphology of the ionic liquid polypyrrole

SEM images of Au2/PPy and Au3/PPY are shown in Fig. 5. The observed surface features are more alike crystals than the polymer particles produced by electropolymerization of pyrrole in water or in other molecular liquids [16] as well as reported for PPy electrosynthesized in BMIMPF$_6$ [17]. The polymer particulates are packed densely on a gold surface, their sizes are larger for the thicker film. The observed chronoamperograms (see Fig.1) of the polymer growth indicate a very slow polymerization process in BMIMBF$_4$, thus, with a presumably predominant contribution of the 2D deposition of the thin polymer film composed of the shorter chains [18]. A smoother, nodular surface structure of polypyrrole synthesized in 1-ethyl-3-methylimidazolium triflate as compared to the polymer prepared in an acetonitrile electrolyte was reported by Sekiguchi et al. [2,3] and the feature was reexamined in the later studies by Deepa and Ahmad [19]. Moreover, the cauliflower like shapes arranged in rows were observed in SEM images for polypyrrole electrodeposited from 1-ethyl-3-methylimidazolium perfluoroethanesulfonimide and atomic force microscopy images showed an array of sub-micron particulates of regular shapes (300-500 nm). Hydrophobicity of the later ionic liquid was considered to effect morphology of the growing polymer film.

Figure 5.

The structure of ionic liquids is known to differ substantially from the structure of conventional molecular liquids. The liquid salts reveal a higher degree of molecular ordering and are sometimes called the nano-structured fluids as they can keep locally a molecular ordering resembling the crystal structure of the solid state salt [20]. The resulting local liquid crystal structure motifs may be copied on the polymer chain arrangement as the later is determined by the anion doping of the oxidized polymer precursor species formed during the

electrooxidative process of pyrrole. The results of single crystal X-ray analysis of the BMIM[+] salts show that the cations and the halogen anions form characteristic column structures [20]. The butyl group rotational isomers of BMIM[+] influences the cation subsystem structures and then the anion subsystem adjust as well. It is likely that the zigzag anion chains found in the crystals of BMINCl exist in the liquid state of the BMIN[+] salts as well. The polypyrrole particles with a geometry of their edges resembling rather crystals than usual round edged cauliflower morphologies may follow from the dominant arrangement pattern of counter-anions in liquid BMIMBF$_4$ at a polymer deposition front.

In addition, SEM micrographs of our polypyrrole layers point out significant influence of thickness and/or the synthesis method on morphology of the surface. A SEM image of Au1/PPy, which was thicker than Au2/PPy and Au3/PPy, and prepared using the potentiostatic deposition step followed by CV deposition step, is shown in Fig. 6. Noteworthy, higher resolution SEM micrographs of Au3/PPy revealed that the microparticles (the largest ones on the surface) are composed of a smaller PPy agglomerates that contain nodular particulates arranged predominantly in a layer by layer fashion.

Figure 6.

3.3. Electrodeposition in BMINBF$_4$–water and testing in BMIMBF$_4$

Water was added to the pyrrole-BMIMBF$_4$ solution to give about equimolar content of water and the salt in the resulting electropolymerization bath. It resulted in a much faster electropolymerization process as compared to the pure ionic liquid process. Components of Fig. 7 compare CV of the two electropolymerization processes taking place at the same electrical conditions of the electrochemical processes. Note the significant IR drop effect for the ionic liquid deposition indicating that conductivity of BMIMBF$_4$ is much lower than conductivity of the BMIMBF$_4$-H$_2$O mixture.

Figure 7.

The two types of polypyrrole electrodes were then characterized by CV and EIS as illustrated in Figs. 8 and 9, respectively. The CV polymer currents recorded in the ionic liquid without added water confirmed a higher yield of polypyrrole prepared with a higher polymerization charge. Therefore, the polymer films (Au1/PPy, Au3/PPy and Au2/PPy) prepared in the first polymerization session can be regarded as thinner (3-4 times) than Au2a/PPy and Au3a/PPy, prepared in the second session. On the other hand, the thinnest film of the second session, Au4a/PPy, has similar thickness to Au2/PPy – the thinnest film of the first session. It is worth to remember that chain length and oxidation degree of polypyrrole was found to decrease with a decrease of the layer thickness [13,18].

Figure 8.

Figure 9.

The impedance data correlate with the CV data indicating an increase of redox capacitance with charge capacity of the film. In general, the impedance spectra of polypyrrole electrodeposited in the pure salt are similar with the spectra of the polymer prepared with water added to the polymerization bath. However, quantitative differences in the parameter values of the model circuit elements might point out structural dissimilarity of the two kinds of the polymer layers (compare data of Table 1 and Table 2). On the other hand, a time parameter of ionic diffusion, B^2, being of the order of seconds corresponds to a diffusion coefficient value of the order of 10^{-8} cm^2/s for the polypyrrole samples monitored at 0.2 V by EIS in dry BMIMBF$_4$ at room temperature, irrespective of their preparation history (Au2a/PPy, Au3a/PPy). It is the similar order of D-values as usually found for ionic diffusion in polypyrrole being in contact with molecular aprotic liquid as propylene carbonate [12] and in water environment where, however, corresponding D-values are often a little bit lower [11]. It should be realized that D-values of the first polymerization session films with thickness of the order of 10^{-1} μm (Au1/PPy, Au3/PPy) would be of the order of 10^{-9} cm^2/s.

Surprisingly, the diffusion time parameter couldn't be determined from EIS of the thinnest film, Au4a. Nevertheless, the characteristic diffusion times B^2, determined in the presented analysis, do not scale with the film thicknesses. The behavior points out a complex and morphology related diffusion paths

Importantly, the double layer impedance parameter n_1 was found to differ for polypyrrole films bearing different polymerization history: $n_1 = 0.7-0.8$ for the films deposited using the BMIMBF$_4$-H$_2$O mixture (Au3a/PPy and Au4a/PPy), $n_1 = 0.6$ for the BMIMBF$_4$ deposited films Au2/PPy, Au3/PPy, Au1/PPy, and Au2a/PPy.

Table 2. Impedance/admittance parameters of polypyrrole electrodes at 0.2 V, prepared by CV in BMIMBF$_4$ (Au2a/PPy) or BMIMBF$_4$-H$_2$O (Au3a/PPy, Au4a/PPy) and measured in BMIMBF$_4$. Thickness order: Au2a/PPy > Au3a/PPy > Au4a/PPy. The CNLS fitting with the electrical circuit model gives χ^2-values of the order of 10^{-4}. Relative errors of parameters are depicted in italics.

Parameter / electrode	Au2a/PPy	Au3a/PPy	Au4a/PPy
R$_0$ / kΩ	1.59 *1%*	0.79 *1%*	0.89 *2%*
R$_1$ / kΩ	3.98 *8%*	5.49 *2%*	0.265 *5%*
Y$_0$(Q$_1$) / Ω^{-1}s^{+n}	6.1·10^{-6} *19%*	3.1·10^{-6} *5%*	1.4·10^{-6} *12%*
n(Q$_1$)	0.58 *4%*	0.78 *1%*	0.69 *1%*
Y$_0$(Q$_2$) / Ω^{-1}s^{+n}	17.·10^{-6} *8%*	20.·10^{-6} *1%*	5.1·10^{-6} *3%*
n(Q$_2$)	0.68 *2%*	0.73 *<1%*	0.84 *<1%*
Y$_0$(T) / Ω^{-1}s$^{+1/2}$	9.9·10^{-6} *5%*	5.5·10^{-6} *6%*	-
B(T) / s$^{1/2}$	1.9 *3%*	1.8 *4%*	-

SEM images of two corresponding polypyrrole layers are shown in Fig. 10.

Figure 10.

Polymerization in the mixed solvent, BMIMBF$_4$-H$_2$O, impacts morphology of the polymer film significantly. Even the reference "dry" BMIMBF$_4$ polypyrrole (Au2a/PPY) does not resemble the thinner films prepared during the first session (Au2/PPy, Au3/PPy, Au1/PPY) when the freshly dried ionic liquid was used. The "dry" ionic liquid was dried a few weeks before use and then kept under nitrogen in a closed container stored in a freezer. This ionic liquid as a solvent for polypyrrole deposition resulted in nodular surface structure of the polymer (see Fig.10 (top)) – generally spherical or irregularly rounded in shape particulates – which is reported as typical morphology for polypyrrole films deposited in different solvents including ionic liquids [16,17,19]. Some trace water present in "dry" BMIMBF$_4$ is reasonable explanation for the difference with freshly dried BMIMBF$_4$. This ionic liquid absorbs water from the atmosphere at a fast rate and strong electrostatic field of ions causes hydration of ions thus reducing electrostatic attraction between BMIM$^+$ cation and BF$_4^-$ anion [21]. Thus the liquid crystal like structure of the solvent is distorted by the water molecules and so distribution of dopant ions at a polymerization front is govern by conformation of the flexible polymer chains leading to rounded cauliflower particulates of the polypyrrole phase.

Polymerization in the mixed BMIMBF$_4$-H$_2$O solvent and subsequent processing in "dry" BMIMBF$_4$ resulted in a specific morphology of polypyrrole films (see Fig.10 (bottom)). Now, polypyrrole films resemble a polydisperse colloid – a dispersion of a solid in a liquid (sol) behaving as a semi rigid mass in which most of the dispersion medium (BMIMBF$_4$) has penetrated into the sol PPy particles forming a gel with some of the dispersed PPy particles

15

visible as islands surrounded by a sea of a rigid liquid. The substantial quantity of water

molecules dissolved in BMIMBF$_4$ (1:1) increases the H$_2$O – H$_2$O interactions thus promoting

hydrophobic interactions and so adsorption of BMIM$^+$ on gold and polypyrrole. Now again

BF$_4^-$ counterions follow the adsorbed BMIM$^+$ pattern that affects arrangement of PPy chains.

Therefore, the molecular BMIMBF$_4$ surfactant layer formed on gold as well as on

electrodeposited polypyrrole is most probably responsible for the specific surface texture of

the polymer layer electrodeposited using pyrrole dissolved in the equimolar BMIMBF$_4$-H$_2$O

mixed solvent. The crystal-like local structure of the ionic liquid must be highly distorted

when the molecular liquid is added. Water added to the BMIMBF$_4$ polymerization solution

was in excess of pyrrole for more than 50 times. Molecular films of water miscible

imidazolium based ionic liquids on glassy carbon electrodes, formed and applied to

electrocatalysis of biological reactants in buffered aqueous solutions, had been already known

[22]. The equimolar BMIMBF$_4$-H$_2$O electrolyte produces the ionic liquid modified Au

electrode by self organization [23]. It seems that the BMIMBF$_4$ electrode film in the mixed

solvent speeds up the polymerization process by preconcentrating of pyrrole at the modified

electrode and causes shorter chains of polypyrrole to dissolve in the ionic liquid. The thinnest

polypyrrole layer studied was observed to cover gold by a transparent film. SEM micrographs

of Au4a/PPy and Au3a/PPy are similar. However, density of the dispersed solid phase PPy

particles is much lower for the thinner Au4a/PPy film (Fig.11) which may be interpreted as

due to the shorter chains of polypyrrole synthesized at the lower potentials [18].

Figure 11.

The physical properties of aqueous solutions of BMIMBF$_4$ were studied thoroughly in

[24]. The conductivity – concentration profiles indicate a high degree of aggregation. This

ionic liquid is water miscible but its hydrophobicity is manifested by surface tension of the

mixture. The surface tension of BMIMBF$_4$-H$_2$O has been shown to be almost constant for the

mixtures containing less than 90% (molar) of water. It means the surfactant properties of

$BMIM^+$ and tendency to form molecular layers of $BMIMBF_4$ at electrodes. This is certainly

the case for our electrodes, Au3a/PPy and Au4a/PPy. Of foremost importance is that no such

substantial differences between the mixed solvent, Au3a/PPy, and the ionic liquid, Au2a/PPy,

electrodes were observed when characterized by CV and EIS.

Besides the surface activity, ionic liquids based on 1-alkyl-3-methylimidazolium salts

in aqueous solution form aggregates that self assembly in a 3D network [25]. The bulk

structure of $BMIMBF_4$ – water mixtures can be of growing importance for morphology of the

thicker films of electrodeposited polypyrrole.

3.4. Elemental analysis of polypyrrole films

Energy dispersive X-ray microanalysis of the electrodeposited polypyrrole films was

undertaken as informative on quantitative elemental composition. The six polypyrrole films

were examined after electrochemical testing in $BMIMBF_4$. Because the composition data

depended on thickness and a surface site of the polymer samples, averaged ratios of elemental

composition corresponding to same spot on the film were considered as reliable enough

analytical information. The element ratio-values were found thickness dependent too.

Therefore, comparisons between the EDX analysis ratio data were considered only for the

films of similar thickness. Influence of the solvent on composition of polypyrrole films was

the most pronouncedly expressed by the F/N atom ratios: 0.9(Au2a/PPy), 2.0(Au3a/PPy),

0.9(Au2/PPy), 1.7(Au4a/PPy). A theoretical F/N value for polypyrrole tetrafluoroborate at the

degree of chain oxidation equal 0.25 is 1.0 while F/N = 2.0 for $BMIMBF_4$. The experimental

values showed explicitly that the equimolar $BMIMBF_4$-H_2O mixture used as the

polymerization solvent resulted in the stable electrode film composed of polypyrrole at least

partially dissolved in the pure ionic liquid $BMIMBF_4$. It confirms the SEM observations on

the colloid semi rigid character of the mixed solvent films.

4. Conclusions

The cyclic potentiodynamic depositions of polypyrrole on gold from pyrrole solutions in $BMIMBF_4$ and in equimolar $BMIMBF_4$-H_2O produced different morphologies of the polymer films. The crystal-like polymer particulates formed compact structures in the dry solvent, whereas the addition of water increased the layer smoothness which resulted from a polydispersive colloid sol/gel semi-rigid state of the film. A cauliflower shaped polypyrrole deposit, which resembles a typical morphology of polypyrrole deposited from molecular solvents, resulted from polymerization of pyrrole that most probably contained traces of water. The substantial content of $BMIMBF_4$ in the colloidal films was proved by EDX analysis of the F/N ratio.

Electrochemical impedance spectra showed a highly distributed character of the charge transport processes in all the studied polypyrrole films. In general, the smaller particulates of polypyrrole prepared in water free ionic liquid were shown to enhance the interfacial ion transfer and to impact the bulk film conductance processes by lengthening the diffusion paths. The higher values of the double layer constant phase impedance parameter $n(Q_1)$ indicate the more electrically homogeneous surfaces of the semi-rigid polypyrrole films obtained from the mixed solvent. The effective ionic diffusion times do not scale with the polymer film thickness. It points out the morphology related diffusion paths.

It was shown using scanning electron microscopy and energy dispersive X-ray microanalysis that the pure $BMIMBF_4$ and mixed $BMIMBF_4 - H_2O$ electrolytes can be used to tailor the micro and nanostructures of electrodeposited polypyrrole. Submicrometer thicknesses corresponding to microgram amounts of the electrodeposited polymer films were compared through cyclic voltammetry and impedance spectroscopy characteristics of polypyrrole.

5. References

[1] J. Rodriguez, H.-J. Grande, T.F. Otero, Polypyrroles: from basic research to technological applications, *in* Handbook of Organic Conductive Molecules and Polymers, H.S. Nalwa (Ed.), Wiley 1997, Vol. 2, p. 415.

[2] K. Sekiguchi, M. Atobe, T. Fuchigami, Electropolymerization of pyrrole in 1-ethyl-3-methylimidazolium trifluoromethanesulfonate room temperature ionic liquid, Electrochemistry Communications 4 (2002) 881.

[3] K. Sekiguchi, M. Atobe, T. Fuchigami, Electrooxidative polymerization of aromatic compounds in 1-ethyl-3-methylimidazolium trifluoromethanesulfonate room-temperature ionic liquid, Journal of Electroanalytical Chemistry 557 (2003) 1.

[4] J. M. Pringle, J. Efthimiadis, P.C. Howlett, J. Efthimiadis, D.R. MacFarlane, A.B. Chaplin, S.B. Hall, D.L. Officer, G.G. Wallace, M. Forsyth, Electrochemical synthesis of polypyrrole in ionic liquids, Polymer 45 (2004) 1447.

[5] M. Armand, F. Endres, D.R. MacFarlane, H. Ohno, B. Scrosati, Ionic-liquid materials for the electrochemical challenges of the future, Nature Materials, 8 (2009) 621.

[6] T. Welton, Room temperature ionic liquids. Solvents for synthesis and catalysis, Chemical Reviews 99 (1999) 2071.

[7] F. Endres, S.Z. El Adedin, Air and water stable ionic liquids in physical chemistry, Physical Chemistry Chemical Physics 8 (2006) 2101.

[8] F. Endres, Ionic liquids: solvents for the electrodeposition of metals and semiconductors, ChemPhysChem 3 (2002) 114.

[9] P. Kubisa, Ionic liquids as solvents for polymerization processes – Progress and challenges, Progress in Polymer Science 34 (2009) 1333.

[10] W. Lu, A.G. Fadeev, B. Qi, E. Smela, B.R. Mattes, J. Ding, G.M. Spinks, J. Mazurkiewicz, D. Zhou, G.G. Wallace, D.R. MacFarlane, S.A. Forsyth, M. Forsyth, Use of ionic liquids for π-conjugated polymer electrochemical devices, Science 297 (2002) 983.

[11] M. Grzeszczuk, G. Żabińska-Olszak, Effects of secondary counterions in the electrochemistry of polypyrrole, Journal of Electroanalytical Chemistry 427 (1997) 169.

[12] P.M. Dziewoński, M. Grzeszczuk, Impact of the electrochemical porosity and chemical composition on the lithium ion exchange behavior of polypyrroles (ClO_4^-, TOS^-, $TFSI^-$) prepared electrochemically in propylene carbonate. Comparative EQCM, EIS and CV studies, Journal of Physical Chemistry B 114 (2010) 7158.

[13] M. Chmielewski, M. Grzeszczuk, J. Kalenik, A. Kępas-Suwara, Evaluation of the potential dependence of 2D-3D growth rates and structures of polypyrrole films in aqueous solutions of hexafluorates, Journal of Electroanalytical Chemistry 647 (2010) 169.

[14] T.deJ. Licona-Sanchez, G.A. Alvarez-Romero, L.H. Mendoza-Huizar, C.A. Galan-Vidal, M. Palomar-Pardave, M. Romero-Romo, H. Herrera-Hernandez, J. Uruchurtu, J.M. Juarez-Garcia, Nucleation and growth kinetics of electrodeposited sulfate-doped polypyrrole: determination of the diffusion coefficient of SO_4^{2-} in the polymeric membrane, Journal of Physical Chemistry B 114 (2010) 9737.

[15] B.A. Boukamp, *in* Equivalent Circuit Users Manual, University of Twente, 1989, Chapter 2, and references therein.

[16] A.F. Diaz, J. Bargon, Electrochemical synthesis of conducting polymers, *in* Handbook of Conducting Polymers, T.A. Skotheim (Ed.), Marcel Dekker 1986, Vol.1, p. 81.

[17] A. Zhang, J. Chen, D. Niu, G.G. Wallace, J. Lu, Electrochemical polymerization of pyrrole in $BMIMPF_6$ ionic liquid and its electrochemical response to dopamine in the presence of ascorbic acid, Synthetic Metals 159 (2009) 1542.

[18] M. Grzeszczuk, M. Chmielewski, Influence of electrodeposition potential on composition and ion exchange of polypyrrole films in aqueous hexafluoroaluminate featured by EQCM molar mass to charge factors, Journal of Electroanalytical Chemistry 681 (2012) 24.

[19] M. Deepa, S. Ahmad, Polypyrrole films electropolymerized from ionic liquids and in a traditional liquid electrolyte: A comparison of morphology and electro-optical properties, European Polymer Journal 44 2008) 3288.

[20] H.-O. Hamaguchi, R. Ozawa, Structure of ionic liquids and ionic liquid compounds: are ionic liquids genuine liquids in the conventional sense, *in* Advances of Chemical Physics, S.A. Rice (Ed.), Wiley 2005, p. 85.

[21] K.R. Seddon, A. Stark, M.-T. Torres, Influence of chloride, water, and organic solvents on physical properties of ionic liquids, Pure and Applied Chemistry 72 (2000) 2275.

[22] P. Yu, Y. Lin, L. Xiang, L. Su, J. Zhang, L. Mao, Molecular films of water-miscible ionic liquids formed on glassy carbon electrodes: characterization and electrochemical applications, Langmuir 21 (2005) 9000.

[23] M. Opallo, A. Leśniewski, A review on electrodes modified with ionic liquids, Journal of Electroanalytical Chemistry 656 (2011) 2.

[24] W. Liu, T. Zhao, Y. Zhang, H. Wang, M. Yu, The physical properties of aqueous solutions of the ionic liquid [BMIM][BF_4], Journal of Solution Chemistry 35 (2006) 1337.

[25] A. Modaressi, H. Sifaoui, M. Mielcarz, U. Domańska, M. Rogalski, Influence of the molecular structure on the aggregation of imidazolium ionic liquids in aqueous solutions, Colloids and Surfaces A: Physicochem. Eng. Aspects, 302 (2007) 181.

Captions of Figures

Figure 1. Chronoamperometric curves of potentiostatic synthesis of polypyrrole at Au substrate electrodes in 0.02 pyrrole molar quotient in BMIMBF$_4$. The "first" means depositions started on a bare Au surface; the chronoamperogram at 1.2V corresponds to deposition of polypyrrole on a polypyrrole electrode prepared in a preceding step.

Figure 2. Progress of polypyrrole deposition on Au2 by the cyclic potentiodynamic method in 0.1M pyrrole -5.3M BMIMBF$_4$.

Figure 3. Third scan cyclic voltammograms of polypyrrole films in BMIMBF$_4$ recorded at potential scan rate 0.05 V/s. Polypyrrole films were electrodeposited on gold electrodes from 0.1 M pyrrole in dry BMIMBF$_4$: —Au1/PPy under successive potentiostatic at +0.9V for 1000s and (-0.65,+1.1)V at 0.05V/s CV regimes, 80 scans, ---Au3/PPy under (-0.55,+1.1)V CV at 0.1V/s, 100 scans, ······ Au2/PPy under (-0.65,+1.1)V CV at 0.1V/s, about 100 scans.

Figure 4. EIS spectra of polypyrrole electrodes in BMIMBF$_4$ at +0.2V: Au2/PPy ■, Au3/PPy ▲, Au1/PPy ●; the full frequency range (10 kHz, 5 mHz) (top), and the low impedance (high frequency) range of the spectra (bottom). The frequency ranges are indicated above the corresponding complex plane plots.

Figure 5. SEM micrographs of the polypyrrole films Au2/PPy (top) and Au3/PPy (bottom), deposited in BMIMBF$_4$ using the cyclic potentiodynamic method.

Figure 6. SEM micrographs of the polypyrrole film Au1/PPy deposited in BMIMBF$_4$ using the initial potentiostatic and final cyclic potentiodynamic deposition steps.

Figure 7. CVs of Au2a/PPy preparation in BMIMBF$_4$ (scans 42 – 100_last) (top), and Au3a/PPY in equimolar BMIMBF$_4$-H$_2$O (scans: 1 – 21_last) (bottom).

Figure 8. Cyclic voltammograms of polypyrrole films in BMIMBF$_4$ recorded at potential scan rate 0.10 V/s. Polypyrrole films were electrodeposited on gold electrodes from 0.1 M pyrrole in: ▬ BMIMBF$_4$ (not freshly dried), under CV at 0.05 V/s in (-0.6,+1.1) V potential

window, number of scans 100, Au2a/PPy (blue); - - - equimolar BMIMBF$_4$-H$_2$O mixture, under CV at 0.05 V/s in (-0.6,+1.1) V potential window, number of scans 21, Au3a/PPy (green); ⋯⋯ equimolar BMIMBF$_4$-H$_2$O mixture, under CV at 0.05 V/s in three successive steps: 1) (-0.6,+0.8) V, number of scans 20, 2) (-0.6,+0.9) V, number of scans 20, 3) (-0.6,+1.0) V, number of scans 20, Au4a/PPy (red).

Figure 9. EIS spectra of polypyrrole electrodes in BMIMBF$_4$ at +0.2V: Au2a/PPy ●, Au3a/PPy ▲, Au4a/PPy ■. The frequency ranges are indicated above the corresponding complex plane plots.

Figure 10. SEM micrographs of Au2a/PPy (top) and Au3a/PPy (bottom) deposited using CV in "dry" BMIMBF$_4$ and equimolar BMIMBF$_4$-H$_2$O, respectively, after redox performance in the former electrolyte.

Figure 11. SEM micrograph of Au4a/PPy film prepared by the three steps CV procedure in equimolar BMIMBF$_4$-H$_2$O and later performing in "dry" BMIMBF$_4$.

Graphical abstract

Polypyrrole electrodeposited from BMIMBF$_4$	Polypyrrole electrodeposited from BMIMBF$_4$-H$_2$O

<50 kHz,5mHz>

Au2
Au2_fit
Au3
Au3_fit
Au1
Au1_fit

Au3 <50kHz, 2.90Hz>
Au1 <50kHz, 0.25Hz>
Au2 <50kHz, 0.77Hz>

Au2
Au2_fit
Au3
Au3_fit
Au1
Au1_fit

30.0kV x5.00k SE   10.0um

30.0kV x5.00k SE   10.0um

30.0kV x30.0k SE   1.00um